Published in final edited form as:
Anal Chem. 2008 September 1; 80(17): 6731–6740. doi:10.1021/ac800823f.

Elimination of undesirable water layers in solid contact polymeric ion-selective electrodes

Jean-Pierre Veder[a], **Roland De Marco**[a], **Graeme Clarke**[a], **Ryan Chester**[a], **Andrew Nelson**[b], **Kathryn Prince**[b], **Ernö Pretsch**[c], and **Eric Bakker**[a]

[a]*Nanochemistry Research Institute, Department of Applied Chemistry, Curtin University of Technology, GPO Box U1987, Perth, Western Australia, 6845, Australia* [b]*Australian Nuclear Science and Technology Organization (ANSTO), PMB 1, Menai, New South Wales, 2234, Australia* [c]*Institute Biogechemistry & Pollutant Dynamics, ETH Zürich, CHN F 16, CH-8092 Zürich, Switzerland*

Abstract

This study aims to develop a novel approach for the production of analytically robust and miniaturized polymeric ion sensors that are vitally important in modern analytical chemistry (e.g., clinical chemistry using single blood droplets, modern biosensors measuring clouds of ions released from nanoparticle tagged biomolecules, lab-on-a-chip applications, etc.). This research has shown that the use of a water repellent polymethyl methacrylate/polydecyl methacrylate (PMMA/PDMA) copolymer as the ion sensing membrane, along with a hydrophobic poly(3-octylthiophene 2,5-diyl) (POT) solid-contact as the ion-to-electron transducer, is an excellent strategy for avoiding the detrimental water layer formed at the buried interface of solid-contact ISEs. Accordingly, it has been necessary to implement a rigorous surface analysis scheme employing electrochemical impedance spectroscopy (EIS), in-situ neutron reflectometry/EIS (NR/EIS), secondary ion mass spectrometry (SIMS) and small angle neutron scattering (SANS) to probe structurally the solid-contact/membrane interface, so as to identify the conditions that eliminate the undesirable water layer in all solid-state polymeric ion sensors. In this work, we provide the first experimental evidence that the PMMA/PDMA copolymer system is susceptible to water "pooling" at the interface in areas surrounding physical imperfections in the solid-contact, with the exposure time for such an event in a PMMA/PDMA copolymer ISE taking nearly twenty times longer than that for a plasticized polyvinyl chloride (PVC) ISE, and the simultaneous use of a hydrophobic POT solid-contact with a PMMA/PDMA membrane can eliminate totally this water layer problem.

INTRODUCTION

Ion-selective electrodes (ISEs) have been used for many years as a reliable method for the analysis of electrolytes in most aqueous media.[1-3] In many applications requiring urgent measurements of ionic activity, ISEs have replaced even the most advanced methods due to their rapid response times and comparable ion selectivities. Such desirable characteristics have made them the centre of considerable attention across many disciplines of science, and they have evolved considerably over the years since the initial design of early ISEs[4-6]. Potential applications of modern ISEs in clinical, environmental and forensic analyses[2, 7-11] have been the driving force for the recent growth in research activity, and it is not surprising that every

j.veder@curtin.edu.au; r.demarco@curtin.edu.au; g.clarke@curtin.edu.au; r.chester@curtin.edu.au; anz@ansto.gov.au; kep@ansto.gov.au; pretsche@ethz.ch; e.bakker@curtin.edu.au.

advance in ISE technology is accompanied by an expectation of lower limits of detection, as well as the potential for miniaturization of the ISE.

A degradation in sensor response with solid-contact ISEs has been associated with the existence of a water layer between the membrane and the solid contact, which behaves unintentionally as an electrolyte reservoir that re-equilibrates on each and every change in sample composition[12, 13]. In recent times, the presence of a hydrophobic conductive polymer or redox mediator, acting as a redox buffering underlayer, has been shown to be important not only for the ion-to-electron transduction process[3, 14], but also for inhibiting the formation of a water layer at the electrode substrate/sensing membrane interface that degrades the response of the ISE[3, 14-17]. Accordingly, solid-contact ISEs should allow an elimination of the liquid contact utilized in conventional polymeric membrane ISEs, along with the concomitant need to control and optimize the filling solution in the liquid contact to achieve low detection limit sensors (see references[18-20]), as well as enabling easy miniaturization of the sensor using a substrate microelectrode.

Miniaturized polymeric ion sensors provide exciting opportunities for the application of these concentration sensitive devices in the detection of ultratrace amounts of total analyte (e.g., attomole quantities[21]), which may also be coupled to novel bioassays utilizing nanoparticle tagged biomolecules[22, 23].

Traditionally, the use of plasticized poly(vinyl chloride) [PVC] as an ion sensing membrane in the absence of an ion-to-electron transducer as the solid contact has been unsuccessful in inhibiting the formation of the detrimental water layer; however, substitution of the PVC ion sensing membrane with a water repellent polymethyl methacrylate/polydecyl methacrylate (PMMA/PDMA) copolymer provides one way of obviating this problem[20]. Furthermore, an extremely hydrophobic conducting polymer solid contact, which is both an ionic and electronic conductor acting as an ion-to-electron transducer[14, 16, 17, 24-26], should be chosen to further mitigate against detrimental water layers in solid contact ISEs. Accordingly, the present investigation evaluates the water repellent PMMA/PDMA copolymer ISE membrane in conjunction with a hydrophobic conjugated (semi-conducting) polymer poly(3-octylthiophene 2,5-diyl) (POT) as an approach for eliminating the water layer in stable and robust solid-contact ISEs. In view of the growing demand for the development of ISEs as microelectrodes for wide and varied applications in analytical science, we hereby describe a systematic and rigorous study of water uptake and water layer formation in hydrophobic solid-state ISEs using electrochemical impedance spectroscopy (EIS), in-situ EIS/neutron reflectometry (NR), secondary ion mass spectrometry (SIMS) and small angle neutron scattering (SANS).

EXPERIMENTAL SECTION

Materials

The following Selectophore Fluka reagents were used in this study: high molecular weight poly(vinyl chloride) (PVC), calcium ionophore IV, silver ionophore IV, sodium tetrakis [3,5-bis(triflouro-methyl) phenyl] borate (NaTFPB), bis(2-ethyl hexyl) sebacate (DOS) and ETH 500 (sourced from Sigma-Aldrich, Castle Hill, New South Wales, Australia). Regioregular poly(3-octylthiophene 2,5-diyl) (POT) was also a Selectophore reagent obtained from Aldrich (Castle Hill, New South Wales, Australia). Analytical grade chloroform was obtained from Selby (Clayton, Victoria, Australia), inhibitor free tetrahydrofuran (THF, 99.8%) was obtained from Sigma-Aldrich and laboratory grade dichloromethane and xylene were obtained from Chem Supply (Port Adelaide, South Australia, Australia). The washing solvents of acetone and ethanol were laboratory grade and obtained from APS chemicals (Seven Hills, New South Wales, Australia) and CSR Distilleries (Nedlands, Western Australia, Australia), respectively. Analytical grade $CaCl_2$ was obtained from Merck (Wangara, Western Australia, Australia)

whilst analytical grade $Ca(NO_3)_2$, ammonia, hydrogen peroxide and KNO_3 were obtained from Ajax Chemical Co (Sydney, New South Wales, Australia). Similarly, analytical grade nitric and hydrochloric acids used in electrode washings were obtained from Ajax Chemical Co. The monomers, methyl methacrylate, 99.5%, (MMA) and n-decyl methacrylate (DMA), 99%, were obtained from Polysciences, Inc. (Gymea, New South Wales, Australia). The polymerization initiator 2,2'-azobis(isobutyronitrile) (AIBN), 98%, was obtained from Aldrich. Ethyl acetate and 1,4-dioxane were reagent grade and obtained from Chem Supply. Milli-Q water was used to prepare all aqueous solutions unless otherwise specified.

Electrochemical Impedance Spectroscopy

Gold substrate electrodes were polished using alumina nanoparticles (300 nm) and copious amounts of water in conjunction with a rotating polishing pad. The electrodes, polishing pads and alumina nanoparticles were all obtained from Metrohm™. After polishing, the electrode was rinsed with large amounts of Milli-Q water and bathed for 5 minutes at a time in acetone, nitric acid (10^{-4}M), MilliQ water and finally dichloromethane. The electrodes were thoroughly rinsed with milliQ water and completely air dried after each cleaning step. The electrodes were subsequently coated with PMMA/PDMA copolymer via a drop casting method involving the casting of 100 μL of the copolymer cocktail directly onto the gold planar disk electrode (3 mm in diameter) within a PEEK plastic body that is 10 mm in diameter. The copolymer Ca^{2+} selective membrane cocktails were made by mixing calcium ionophore IV (1 wt%), ETH 500 (1.1 wt%), NaTFPB (0.5 wt%), PMMA/PDMA copolymer (97.4 wt%) and dichloromethane (1 mL per 100 mg of membrane components) and finally sonicating for ten minutes to degas the mixture prior to casting of the membrane. Synthesis of the PMMA/PDMA copolymer has previously been reported by Qin et al.[27] For the electrodes utilizing an underlying conducting polymer, prior to the casting of the copolymer membrane, a POT cocktail was cast directly onto the electrode substrate for a total of 6 times using volumes of 10 μL in each casting. The POT cocktail was prepared by dissolving 0.94 mg of POT into 20 mL of chloroform.

EIS studies were undertaken on an EG & G Princeton Applied Research Model 273A electrochemical impedance analyzer. Due the low conductivity in the copolymer membranes, in order to increase the signal to noise ratio, all EIS spectra were collected using an excitation potential of 100 mV root mean square (rms), and a frequency range of 100kHz-1mHz utilizing 4 point data averaging statistics. Using a conventional three electrode cell, the EIS experiment was maintained at 20 ± 1°C and contained 0.1M solution of $CaCl_2$ for all measurements. A Metrohm™ Au-tip ISE working electrode, a platinum counter electrode and a silver/silver chloride Orion™ double junction reference electrode were used in the measurements.

Electrochemical Impedance Spectroscopy/Neutron Reflectometry

NR was carried out at the facilities of the Australian Nuclear Science & Technology Organization (ANSTO) using the instrument located in the HIFAR reactor. The instrument and experimental conditions for NR measurements have been reported previously[28]; however, the research conducted here was collected over the Q range of 0.005−0.4 $Å^{-1}$. The Teflon-based solid-liquid NR cell used for D_2O/H_2O contrast measurements has also been reported previously by James *et al*.[29]

For the EIS portion of the in-situ measurements, a Princeton Applied Research Parstat 2263 portable potentiostat was used. The NR cell was modified slightly to accommodate the positioning of EIS electrodes by using a doped silicon wafer as a low resistance working electrode, as well as platinum counter electrode and platinum pseudo reference electrode, which were all screwed into the filling ports of the original NR cell. The molecularly thin copolymer films had much lower impedances than the usual macroscopic electrodes, thereby EIS data could be collected using an excitation potential of 10 mV rms, and a frequency range

of 100 kHz-10 mHz with only one point data averaging. A 1 M solution of KNO_3 was always used as the analyte, regardless of the solution type, whether D_2O, H_2O or a mixture of D_2O/H_2O, so as to provide a modest solution resistance between the 10 cm diameter silicon wafer and the counter and auxiliary electrodes. Measurements were commenced only after the sample stage had been aligned correctly with reference to the neutron beam.

The doped and atomically flat silicon wafers were used as received as the working electrodes since they had been pre-polished to about 1 Å rms roughness [as obtained from Crystran LTD (Poole, Dorset, UK)]. The silicon was initially covered with 5−10 mm of excess xylene and placed on a hotplate at a temperature of 150°C for 1−2 hours. The wafer was then rinsed with ethanol and water prior to placement in RCA-1 solution. The RCA-1 solution comprised a 5:1:1 volume ratio of water: ammonia: hydrogen peroxide. The solution was then put on a hotplate at a temperature of 150 °C for a minimum of 20 minutes. The wafer was rinsed again with water and placed in a RCA-2 solution comprising a mixture of 6:1:1 volume ratios of water: HCl: hydrogen peroxide. This solution was left on a hotplate at the same temperature as previously mentioned for a minimum of 20 minutes. This cleaning procedure was followed by rinsing in water and 10 minutes in 0.1 M ammonia solution at room temperature, followed by a water bath for 5 minutes. The cleaning procedure is said to produce a hydrophilic surface, leaving a relatively dense layer of Si-OH groups on a silicon oxide layer.[30]

Xylene was chosen as the solvent for spin casting of the membrane onto the wafer due to its lower volatility compared to dichloromethane which had a tendency to deposit more of the polymer in the centre and outer rim of the silicon wafer after spin casting. A solution of POT was made up in xylene with a composition of 0.34 %(w/v). A 1.5 %(w/v) solution of the copolymer was then made up by mixing the copolymer (97.6 wt%), NaTFPB (0.6 wt%), silver ionophore IV (1.8 wt%) together with xylene in appropriate quantities. Note, in this experiment, unlike the others with a calcium ionophore, a silver ISE was used since the preliminary NR modeling, planning and beamtime proposal had considered this membrane composition. Notwithstanding, it is possible to undertake the NR technique using any ionophore, and the properties under investigation in this study (i.e., comparable membrane nanostructure in the presence and absence of water) will not vary in the presence of different ionophores. One electrode was prepared by spin coating the copolymer cocktail directly onto the wafer at 3500 rpm. Another electrode was prepared in the same way; however, an underlayer of POT was applied also via the spin coating method at 3500 rpm. Each of the electrodes were annealed in a vacuum oven at 80 °C and a pressure of 0.1 mmHg for 20 hours to relieve localized stresses in the spin cast film surface.

Note that all data obtained via NR was modeled using the customized NR software, IGOR Pro-Motofit (Wavemetrics, Lake Oswego, Oregon, USA)[31], and NR studies were performed on the “as prepared” samples of the copolymer spin cast onto the silicon wafer, and the POT/copolymer combination that was spin coated in the same manner.

Secondary Ion Mass Spectrometry

In this experiment, rectangular gold sheets (5 mm wide, 10 mm long and 0.5 mm thick) were used as the ISE substrates, and polymer cocktails were cast onto the coupon after the aforesaid surface preparation technique. Identical polymer cocktails to those used in EIS analyses were employed; however, the cocktails were diluted 10-fold and cast onto the gold coupon in a volume of 44.3 μL, so that the approximate thickness was 8 μm, so as to allow water permeation to the substrate electrode over 48 hours. One of two copolymer ISEs was submerged in 0.1M NaCl whilst the other was submerged into 0.1M $Ca(NO_3)_2$ solution for 48 hours. The treated ISEs were taken out of solution and rinsed in Milli-Q water. The copolymer was then scraped back to reveal the gold contact. Elemental mapping was carried out on the straight gold contact since the gold contact did not require a conductive coating for charge neutralization during

SIMS analyses. All SIMS images were collected on a Cameca IMS 5f dynamic SIMS instrument. A 10 keV Cs^+ primary ion source, with a beam current of 0.3 nA, was used to generate negative secondary ion images for a number of species including ^{23}Na and ^{35}Cl. The primary beam, with a diameter of ~ 3 μm, was rastered over an area of 250 × 250 μm during all SIMS imaging measurements. The images collected from the treated ISEs were compared to images collected from a gold control sample that had not been bathed in solution.

Small Angle Neutron Scattering

The work undertaken for SANS was based closely on the work of Ye et. al.[32], employing time dependent studies of polymers that were bathed in a heavy water solution for several hours. The SANS experiments were performed using the instrument housed at ANSTO's Lucas Heights laboratory, and the following experimental conditions were employed; wavelength λ = 5 Å, detector position 5000 mm from the sample, beamstop size 45 mm, source aperture 35 mm, q range 0.01−0.12 $Å^{-1}$, detector offset 0 mm and sample aperture 10 mm. The scattering patterns were corrected for transmission; spectrometer background and cuvette scattering, in addition to this were converted to absolute scattering cross section units using an A3 silica standard of known incoherent scattering. Data analysis was undertaken using the Igor Pro software package and the SANS data analysis macros written at NIST[33]. The PVC membranes were combined by adding PVC (33.1 wt %), DOS (66.3 wt %) and NaTFPB (0.6 wt %) together with 5ml of THF and poured into glass rings of 23 mm internal diameter. The THF was allowed to evaporate prior to putting the membranes into the SANS cuvettes. The copolymer membrane that had been previously synthesized (20 wt % MMA and 80 wt% DMA) was placed into the SANS sample holders without further treatment. The PVC membrane was initially placed into a dry cell cuvette and measured several times, with each measurement lasting 20 minutes. The PVC membrane was placed into a wet-cell cuvette and surrounded with 10^{-2} M HNO_3 in D_2O to test for the effect, if any, of the migration of ions from solution into the membrane and measurements were carried out at 20, 60, 120, 200 and 300 minutes after the addition of heavy water, with each measurement lasting for 10 minutes. The PMMA-PDMA co-polymer was placed in a wet-cell cuvette and measured dry 17 times with each measurement lasting for 10 minutes. D_2O was then placed in the cell to surround the co-polymer. Measurements were then taken at 60, 120, 180, 600 and 1500 minutes after the heavy water addition. All sample holders were quartz with a 2 mm optical path length.

RESULTS AND DISCUSSION

Several state-of-the-art surface analysis and electrode kinetic techniques have been used here to study the buried interfaces of solid-contact ISEs. First, EIS has been chosen since it is a powerful electrode kinetic technique that will provide in depth information about the dielectric properties of the solid contact sensors, particularly the influence of continuous waters layers and pockets of water in pores and “pin holes” in the solid contacts, on the contact resistance at the solid contact/ion sensing membrane interface. Second, *in-situ* electrochemical NR has been selected since it is an excellent nanocharacterization technique that will allow a real-time investigation of the evolution of water layers in solid contact ion sensors as a function of the chemical and physical factors that control the formation of water layers, and will complement and validate the EIS data, noting that a combination of EIS and NR will provide a powerful electrode kinetic/nanocharacterization technique. Next, SANS has been used to conduct in-situ real-time studies of the sorption of water into the polymeric ISE films, thereby deriving important information about the permeability of water into membranes and its concomitant effect on the formation of water layers in solid-contact ion sensors. Last, *ex-situ* high sensitivity SIMS depth profiling and imaging enabled a detection of subatomic percentages of ionic species in the 1−100 nm depth and 3 μm spot sizes or 250 × 250 μm raster areas of the buried interfaces allowing a monitoring of salt residues at the ISE membrane/solid contact interface

when a water layer is prevalent. Essentially, this conglomeration of information will provide detailed insights into the implications of water sorption and transportation in water repellent copolymer solid contact ISEs, enabling the development of a robust methodology for the fabrication of new and improved solid-contact sensors.

Electrochemical Impedance Spectroscopy of the Ca^{2+} Selective Electrode

Unpublished research on a double membrane incorporating a solid-state chloride ion-exchanger glued to a plasticized PVC Ca^{2+} ISE revealed that the high frequency semicircle attributable to the bulk membrane resistance of the double membrane exceeded significantly - by 20% - the additivity of the bulk resistances of the chloride ion-exchanger and Ca^{2+} ISE, noting that this outcome is symbolic of a contact resistance at the interface between the two substrates. Upon continuous exposure to an aqueous electrolyte, the composite value for the high frequency bulk membrane and contact resistance eventually diminished by about 15%, and this is attributed to a wetting of the buried interface by transported water and electrolyte, thereby diminishing the contact resistance. Notably, the bulk membrane resistance of a double membrane including two individual Ca^{2+} ISEs revealed, to within the limits of uncertainty with EIS (i.e., a few %), congruence with the additivity of the individual bulk membrane resistances, and the high frequency semicircle of the double membrane did not show a diminution in resistance upon continuous exposure to electrolyte. This provides credence for the interpretation of a poor solid contact yielding a contact resistance that, when wetted by water and transported ions, is symbolic of the formation of a water layer at the buried interface.

The EIS response of all systems were modeled using ZSimpWin Version 2.00 software[34], and an equivalent circuit (see Figure 1) was used in the circuit modeling. Figures 2a and 2b present EIS Nyquist plots for a copolymer Ca^{2+} ISE and a POT/copolymer Ca^{2+} ISE immediately after drop casting and following continuous exposure in 10^{-2} M $CaCl_2$, respectively. In both cases, the EIS spectra revealed two distinct time constants; one located at high frequency and the other at low frequency. The high frequency time constant (i.e., R_B and Q_B) is associated with the bulk membrane resistance of the ISE coupled to the contact resistance at the buried interface (i.e., membrane-contact resistance) in parallel with the combined geometric capacitance. The low frequency time constant (i.e., R_{IT} and Q_{IT}), on the other hand, is a direct result of the double layer capacitance of the ISE system and the charge transfer resistance at the interface between the aqueous electrolyte and the copolymer or POT/copolymer ion-selective membrane.[14] It is important to note that a third high frequency EIS time constant for the POT underlayer, as detected in a seminal paper by Bobacka et al.[35], was unable to be resolved due presumably to its minute resistance (tens to hundreds of Ω) relative to the much higher membrane resistance of the PMMA/PDMMA copolymer (i.e., 100−400 MΩ).

As the electrode is bathed in solution, it is evident that the high frequency semi-circle, indicative of the time constant for the membrane-contact resistance, increases due to an elevation in the membrane resistance. This is due presumably to the reported phenomenon of ion trapping of hydrophilic and ionic impurities within water droplets in the membrane due to water uptake[32, 36-39]. Furthermore, the hydrophilic or ionic impurities in the membrane assist in the formation of water deposits, or small droplets, which would subsequently raise the membrane resistance due to a reduced ion-exchange capacity through ion trapping, and it is expected that the resistance of the membrane will continue to rise until the membrane has equilibrated with water. It is evident from the Nyquist plot in Figure 2a and the bulk membrane-contact resistance values in Table 1 that the copolymer ISE shows a continual rise in membrane resistance until 460 hours followed by a sharp decline in the bulk membrane-contact resistance after this period due presumably to the formation of a water layer that acts as a low-resistance shunt by wetting the buried interface with transported water and ions. Note that this experiment has been repeated on 3 separate occasions yielding similar EIS responses, and the results

presented herein are indicative of the observed effect. This has important ramifications for solid-contact ISEs in view of the fact that, until now, it was hypothesized that the water repellent copolymer would inhibit the formation of a water layer. Nevertheless, it is apparent that, when compared to a similar PVC ISE system, the formation of a water layer in a copolymer ISE occurs at a phenomenally slower rate, requiring over twenty times longer than a normal PVC ISE (this ratio has been estimated by comparing the water saturation rate in a PVC ISE of about 20 hours[40] with that of a copolymer ISE of around 460 hours). Such a characteristic is extremely desirable for the fabrication of robust and reliable ISEs to be used in measurements over long periods before the sensor response is degraded. When coupled with an underlayer deposit of hydrophobic POT, the copolymer ISE exhibits an extremely steady response eventually coming to equilibrium after approximately 450 hours, as evident in Figure 2b and Table 2, with no indication of the formation of a water layer, i.e., no diminution in the bulk membrane-contact resistance arising from wetting of the solid-contact/membrane interface.

In-Situ Electrochemical Impedance Spectroscopy/Neutron Reflectometry of a Ag^+ Selective Electrode

With NR, it is necessary to prepare molecularly thin and atomically flat films [tens to hundreds of Å in thickness and a few Å rms in roughness], so as to enable sufficient reflectivity (via reduced roughness) and to minimize the number of interference fringes arising from the coherent neutron scattering of successive layers of polymeric material (through diminished thickness) in the thin film. If the prerequisites are satisfied then it is possible to derive atomic scale information about the physical nature of thin films. Previous work on plasticized PVC membranes revealed that, for perfectly resolved and atomically flat layers, a water layer produces a series of interference fringes that are interspersed with the corresponding interference fringes for the ISE film, thereby confirming that NR can be used to detect water layers in solid-contact ISEs[40]. Significantly, NR was used in 2008 to characterize successfully the formation of a water-layer at the solid contact/ISE membrane interface in coated-wire ISEs[40], and an excellent paper in J. Am. Chem. Soc. in 2004 reported on the successful application of NR in combination with cyclic voltammetry to monitor changes in the nanostructures of oxidized and reduced thin films of polyvinylferrocene[41].

X-ray reflectometry (XR) was used to characterize the thickness and roughness of the ISE films to ensure that the films were of sufficient integrity for NR characterization. The high definition in the interference fringes to Q values of 0.4 $Å^{-1}$ is indicative of an atomically smooth film, noting that the copolymer ISE layer was found to be 313.4 Å in thickness with a roughness of 4.5 Å. XR measurements also showed that the POT/copolymer ISE membrane [see Figure 3a & 4a for XR reflectivity and scattering length density (SLD) plots] had a comparable thickness to that of the copolymer membrane without POT.

An interesting observation from the results of the NR and XR measurements on the POT/copolymer system (see Figure 3b, c & d, Table 3 and Figure 4b, c & d) was that the SLDs of the POT underlayer and the PMMA/PDMA copolymer were very similar, as evidenced by SLDs measured on straight copolymer and POT/copolymer films, making it very difficult to differentiate between the two layers. Notwithstanding, the observed roughening of the POT/copolymer interface symbolizes that there may have been an amalgamation of the two layers during the spin casting of films from a xylene solvent. The POT itself was seen to have an initial mean thickness of 42.9 Å, whilst the copolymer had a thickness of 295.8 Å.

Upon measuring the second contrast of the D_2O and H_2O mixture, it appears that the copolymer and POT layers may have expanded beyond their primary dimensions due to water uptake in the membrane; however, the change in thickness is within the bounds of experimental uncertainty using NR (i.e., a few percent). This was evidenced by the slight variation in SLD values, whereby the polymer membranes become further hydrated over the course of bathing

in each neutron scattering contrast. The third and final contrast in straight H_2O showed a lack of detail due to contrast matching between the POT/copolymer membrane and the H_2O electrolyte. Nevertheless, in all neutron scattering contrasts, it was evident that there was no distinct formation of a water layer within the membrane. In-situ EIS data obtained concurrently with the NR measurements confirmed the lack of a water layer since the POT/copolymer ISE did not reveal the characteristic diminution in membrane-contact resistance ascribable to wetting of the buried interface, as seen in the Nyquist plot in Figure 5 and the data in Table 4, showing an equilibration of the EIS response after approximately 9 hours of exposure to solution. It is significant to note that previous EIS results on a POT/copolymer ISE revealed that it took approximately 460 hours for a 90 μm film to allow the transportation and equilibration of water (see Figure 2), while the present EIS results on a 31 nm film expectedly scaled by a factor of approximately 10^4 for the molecularly thin film, noting that the film properties do not scale linearly for molecularly thin layers since it has been found that these films display quantum confinement effects (unpublished data). As expected, the EIS data was fitted successfully to the same equivalent circuit as the one used for the macroscopic ISE (see Figure 1).

In the absence of POT, the Ag^+ selective copolymer ISEs exhibited qualities that suggested the formation of a water layer at the solid-contact/ion sensing membrane interface. EIS revealed the formation of a water layer after 31 hours in solution. This is indicated by the reduction in the bulk membrane resistance (see Table 5), caused by the dramatic reduction of the contact resistance at the solid-contact/ion sensing membrane due to the water layer (again, yielding an expected time scaling factor of about 10^4). In the instance of the PMMA/PDMA copolymer system without the use of a conducting polymer underlayer (data not shown), the modeled data showed a severe interfacial roughening that became more pronounced on extended soaking in solution that can only be ascribed to the formation of “pockets and pools” of localized water that deposited out of the polymer and remained either within the membrane or gathered around imperfections at the solid contact/ISE membrane interface. The formation of water “pockets and pools”, as opposed to a well defined water layer, makes it difficult to model the NR data due to the fact that NR is suitable only for well defined and atomically flat films. Such a task, involving the investigation of the formation of inhomogeneities due to the uptake of water by the membrane requires a sub-surface analytical technique such as SANS that is described later. It is presumed that, if the ISE is left for a lengthy period of time in solution, these “pockets and pools” of water will eventually evolve into a well-defined water layer at the interface.

Surface Studies of Ca^{2+} Ion-selective Electrodes

A SIMS surface study was undertaken on gold coupons that had been coated with 8 μm thick copolymer membranes that had been exposed to 0.1 M $Ca(NO_3)_2$, 0.1 M $CaCl_2$ or 0.1 M NaCl for 48 hours. Importantly, the membrane thickness had been scaled back to enable the transportation of water through the membrane in 48 hours, noting that EIS had shown that a 90 μm layer took approximately 460 hours to equilibrate with the electrolyte (see Figure 2).

When the copolymer was scraped back to reveal the exposed gold/membrane interface, $Ca(NO_3)_2$, $CaCl_2$ or NaCl residues were not detected on the solution treated surfaces as evidenced by a lack of excess SIMS signals for calcium, nitrogen, chlorine, sodium and oxygen as compared to the background levels of a control gold specimen (results are not shown). It was suspected that this could be due to one or a combination of two main reasons. The first reason could be that scraping the copolymer back may have removed the evidence of salt formation, and although this is possible, the salts would have been pushed back with the copolymer, thereby providing a calcium excess along the scraped edge, noting that this effect was not evident in SIMS imaging of the scraped edge. Alternatively, salts could have been present in minute quantities in highly localized regions, as suggested by the NR data that showed that the

copolymer had a tendency to form “pockets and pools” of water rather than a well defined water layer like the one formed with the PVC ISE, and these deposits could not be detected in the 250 × 250 μm raster spots employed in SIMS depth profiling.

Upon failing to detect significant amounts of salt residues at the gold contact/ISE membrane interface using SIMS depth profiling, SIMS elemental mapping was employed to obtain a visual representation of where, if at all, the salts had deposited at the gold/membrane interface. After rastering the surface for a very short period to sputter away any surface contamination, elemental maps were taken on the sample exposed to $Ca(NO_3)_2$, as well as the sample exposed to NaCl. Most significantly, “hot spots” of sodium and chloride appeared in the sample that was bathed in the sodium chloride electrolyte. Although the chlorine data might be susceptible to line interferences from other elements, the maps consistently showed portions of the sample that contained sodium ions (free of ion interferences) as well as chloride ions in the same location, indicating that there was an accumulation of NaCl from the bathing solution that had deposited at the interface (see Figure 6). This outcome is internally consistent with the presence of “pockets” or “pools” of water, as had been revealed previously in the NR/EIS study.

Due to the difficulty in detecting localized zones of deposited ions with the straight PMMA/PDMA copolymer ISE, the authors did not attempt a comparable SIMS study on a POT/copolymer solid-contact ISE since it is known that this system does not allow the formation of a water layer[20].

Small Angle Neutron Scattering

The SANS data on PVC membranes incorporating DOS as a plasticizer are in excellent agreement with results obtained by Ye *et al.*[32] who showed a well-defined peak in the neutron scattering data that is indicative of nanocrystalline inhomogeneities dispersed within the membrane. Figure 7a reveals a peak at a scattering vector value or $Q \approx 0.03$ Å^{-1}, as well as the influence of prolonged exposure in a D_2O electrolyte. As was also shown by Ye *et al.*[32], the SANS curves overlap to near perfection at high Q values; however, the effects of soaking in D_2O are clearly evident at lower Q values or larger nanoscatterer sizes in the membrane since Q is inversely proportional to the size of scatterers. Most probably, the effects associated with soaking of the polymer in the D_2O solution are due to the formation of water nanodroplet inhomogeneities in the membrane[36-39], as evidenced by the asymptotically decaying portion of the scattering peak. The highest Q-value at which water inhomogeneities begin may be related directly to the radius of gyration[42], given by $R_g q_{min} \geq 5$; hence, by using the maximum Q-value (which is 0.02 Å^{-1}), we obtain $R_g \geq 25$ nm. Essentially this means that the water inhomogeneities within the membrane are ≥ 25 nm in size. The influence of membrane bathing in dilute HNO_3 demonstrated that water nanodroplet formation is not affected by the co-extraction of HNO_3.

When compared with the SANS spectra for the copolymer (see Figure 7b), it is evident that the copolymer lacks a well defined peak, nor does it contain any time resolved effects at low Q values as a consequence of water uptake within the membrane. This effectively means that, unlike a plasticized PVC membrane, the structure in the copolymer membrane is inconsistent with inhomogeneities or a detection of neutron scattering contrast against the surrounding polymer matrix. This is not to say, however, that minute amounts of nanocrystalline inhomogeneities do not exist in the copolymer, but more simply that none are detectable by SANS. Nonetheless, the SANS data coupled with the results from EIS, in-situ NR/EIS and SIMS demonstrated an absence of water nanodroplets via the absorption of water. This implies that the copolymer membrane, unlike a plasticized PVC membrane, exists in an entirely plasticized state (despite containing no plasticizer), and displays little or no propensity for water uptake as a consequence of its water repellent nature. Note, the absence of nanocrystallites is expected since the copolymer's glass transition temperature is well below room temperature.

Physical Models for PVC and Copolymer ISE systems

Although it is not possible to unequivocally characterize a complex interfacial system like solid-contact ISEs using any of these materials characterization methods alone, a combination of techniques such as EIS, in-situ NR/EIS, SIMS and SANS is able to identify the reasons for decreased stability and high sensor drifts after prolonged exposure of the solid-contact sensor to an electrolyte. Figures 8a and 8b illustrate the effect of water uptake in a PVC ISE and a PMMA/PDMA copolymer ISE, respectively, as evidenced by this multi-technique materials characterization approach. As in Thomas's model[36, 43], it is proposed that water diffuses through the membrane phase, in which it is slightly soluble, and forms small water droplets at impurity sites within the membrane. The difference in the osmotic pressure between the external solution and the water droplets, may cause additional water to diffuse through the membrane forming water droplets that grow and deform[36]. As a result of this multi-technique characterization approach, an extension can be made on this theory, whereby water nanodroplets deposited at the buried interface continue to grow until a complete molecularly thin layer of aqueous solution is formed. For a PVC system, this phenomenon requires only a small amount of time due to the poor adhesion properties at the solid-contact along with the membrane's relatively high propensity for water absorption and transportation forming a continuous water layer (see Figure 8a), whereas the copolymer requires far more time (up to 20 times longer than a PVC system) due to its physically robust nature, good adhesion properties and water repellent nature. Significantly, the diffusion coefficients of ions in methacrylic-acrylic acid ISE membranes are about 2 orders of magnitude lower than the corresponding values in plasticized PVC membranes[44], and the presently observed rate of water transportation in the copolymer film (about 20 times slower than PVC) are internally consistent with the previously published diffusion data on such membranes. Despite the positive attributes of the PMMA/PDMA copolymer, it is likely that localized “pockets and pools” of water are formed in areas surrounding physical imperfections at the electrode/membrane interface. The physical model in Figure 8b demonstrates this concept showing that the copolymer system experiences the same water uptake mechanism as a PVC membrane; however, it occurs to a much lesser extent. By contrast to a PMMA/PDMA copolymer system that forms “pools” of water, a PVC membrane eventually forms a well-defined water layer.

When a hydrophobic POT solid-contact is used in conjunction with the water repellent copolymer (see Figure 8c), the NR data suggest that the copolymer and the POT amalgamate to some extent which undoubtedly inhibits water layer formation at the buried interface. Figure 8c also shows that miscible water as well as small water droplets enter the copolymer membrane, but to a lesser extent than in a PVC membrane. The slight merging of the POT and copolymer layers thereby inhibit water uptake completely at the solid-contact/membrane interface leaving an underlayer of pure POT, provided that the film integrity is of an excellent quality.

An excellent 2008 review by Lindner and Gyurcsanyi[45] has addressed the deleterious effects of an unintentional water layer on the analytical performance of solid-contact polymeric ISEs. It is known that the unintentional water layer equilibrates with membrane-transported species (e.g. CO_2 and O_2[46-48], as well as primary and interfering ions[13, 20]), changing the chemistry at the backside of the ISE membrane, along with the concomitant sensor response characteristics (i.e., deteriorated selectivity, detection limit and drift rate) by at least an order of magnitude[20].

CONCLUSIONS

This study presented the first experimental evidence for the low propensity for water absorption and transportation in the PMMA/PDMA copolymer ISE, thereby eliminating the formation of a detrimental water layer at the ion-sensing membrane/solid-contact interface. Previous studies

of the copolymer's propensity for water layer formation were not conducted over a long enough period to enable the mass transportation of water through the water repellent copolymer membrane. Although the sole use of copolymer gives extremely steady response and exhibits a relatively long lifetime compared to a conventional solid-contact//PVC ISE, the use of a hydrophobic POT solid-contact in conjunction with a water repellent copolymer membrane conspires to eliminate the water layer altogether. This provides an ideal strategy for the fabrication of robust and reliable solid-contact ISEs that are miniaturizable for applications in many fields of contemporary research. Nevertheless, it is extremely important to note that physical imperfections in the POT underlayer such as pores and pinholes will act as repositories for localized pools of water. Accordingly, it is necessary to produce high quality POT films in solid-contact ISEs, and we are presently undertaking research to develop high integrity POT films, on a nanoscale, using a variety of techniques such as electropolymerization (see the early electropolymerization work by Bobacka et al.[35]) and spin casting as a means of providing a robust technology platform for the production of a new generation of high quality solid-contact ISEs.

ACKNOWLEDGMENTS

The authors acknowledge the financial support of the Australian Research Council (LX0454397 and DP0665400), Australian Institute of Nuclear Science and Engineering, the National Institutes of Health (EB002189) and the Swiss National Foundation. We also thank Mr. Armand Atanacio at ANSTO for assistance with the SIMS research.

REFERENCES

1. Bakker E, Buhlmann P, Pretsch E. Electroanalysis 1999;11:915–933.
2. Bakker E, Diamond D, Lewenstam A, Pretsch E. Anal. Chim. Acta 1999;393:11–18.
3. Michalska A. Anal. Bioanal. Chem 2006;384:391–406. [PubMed: 16365779]
4. Cattrall RW, Drew DM, Hamilton IC. Anal. Chim. Acta 1975;76:269–277.
5. Cattrall RW, Freiser H. Anal. Chem 1971;43:1905–1906.
6. Cattrall RW, Hamilton IC. Ion-Sel. Electrode Rev 1984;6:125–172.
7. Bakker E, Pretsch E. Anal. Chem 2002;74:420A–426A. [PubMed: 11811417]
8. Bakker E, Pretsch E. TrAC, Trends Anal. Chem 2001;20:11–19.
9. Bakker E. Anal. Chem 2004;76:3285–3298. [PubMed: 15193109]
10. Lewenstam A, Maj-Zurawska M, Hulanicki A. Electroanalysis 1991;3:727–734.
11. Konopka A, Sokalski T, Michalska A, Lewenstam A, Maj-Zurawska M. Anal. Chem 2004;76:6410–6418. [PubMed: 15516135]
12. Bakker E, Pretsch E. TrAC, Trends Anal. Chem 2005;24:199–207.
13. Fibbioli M, Morf WE, Badertscher M, De Rooij NF, Pretsch E. Electroanalysis 2000;12:1286–1292.
14. Bobacka J. Anal. Chem 1999;71:4932–4937.
15. Bobacka J. Electroanalysis 2006;18:7–18.
16. Migdalski J, Blaz T, Lewenstam A. Anal. Chim. Acta 1996;322:141–149.
17. Bobacka J, Ivaska A, Lewenstam A. Electroanalysis 2003;15:366–374.
18. Chumbimuni-Torres KY, Rubinova N, Radu A, Kubota LT, Bakker E. Anal. Chem 2006;78:1318–1322. [PubMed: 16478128]
19. Sutter J, Lindner E, Gyurcsanyi RE, Pretsch E. Anal. Bioanal. Chem 2004;380:7–14. [PubMed: 15309365]
20. Sutter J, Radu A, Peper S, Bakker E, Pretsch E. Anal. Chim. Acta 2004;523:53–59.
21. Malon A, Vigassy T, Bakker E, Pretsch EJ. Am. Chem. Soc 2006;128:8154–8155.
22. Chumbimuni-Torres KY, Dai Z, Rubinova N, Xiang Y, Pretsch E, Wang J, Bakker EJ. Am. Chem. Soc 2006;128:13676–13677.
23. Thurer R, Vigassy T, Hirayama M, Wang J, Bakker E, Pretsch E. Anal. Chem 2007;79:5107–5110. [PubMed: 17530777]

24. Michalska A, Dumanska J, Maksymiuk K. Anal. Chem 2003;75:4964–4974.
25. Michalska A. Electroanalysis 2005;17:400–407.
26. Bobacka J, Lindfors T, McCarrick M, Ivaska A, Lewenstam A. Anal. Chem 1995;67:3819–3823.
27. Qin Y, Peper S, Bakker E. Electroanalysis 2002;14:1375–1381.
28. Nelson A, Muir B, Oldham J, Fong C, McLean K, Hartley P, Oeoiseth S, James M. Langmuir 2006;22:453–458. [PubMed: 16378459]
29. James M, Nelson A, Schulz JC, Jones MJ, Studer AJ, Hathaway P. Nucl. Instrum. Methods Phys. Res., Sect. A 2005;536:165–175.
30. Carim AH, Dovek MM, Quate CF, Sinclair R, Vorst C. Science 1987;237:630–633. [PubMed: 17758564]
31. Nelson AJ. Appl. Crystallogr 2006;39:273–276.
32. Ye Q, Borbely S, Horvai G. Anal. Chem 1999;71:4313–4320.
33. Kline SR. J. Appl. Cryst 2006;39:895–900.
34. Yeum, B. In: Equivalent Circuit, Users Manul. EChem Software. 2nd Ed.2001.
35. Bobacka J, McCarrick M, Lewenstam A, Ivaska A. Analyst 1994:1985–1991.
36. Li Z, Li X, Petrovic S, Harrison DJ. Anal. Chem 1996;68:1717–1725.
37. Harrison D, Li X, Petrovic S. ACS Symp. Ser 1992;487:292–300.
38. Li Z, Li X, Petrovic S, Harrison DJ. Anal. Methods Instrum 1993;1:30–37.
39. Chan AD, Harrison DJ. Anal. Chem 1993;65:32–36.
40. De Marco R, Veder JP, Clarke G, Nelson A, Prince K, Pretsch E, Bakker E. Phys. Chem. Chem. Phys 2008;10:73–76. [PubMed: 18075683]
41. Cooper JM, Cubitt R, Dalgliesh RM, Gadegaard N, Glidle A, Hillman AR, Mortimer RJ, Ryder KS, Smith EL. J. Am. Chem. Soc 2004;126:15362–15363. [PubMed: 15563146]
42. Porod, G. In: Small Angles X-ray Scattering. Academic Press; London, U.K.: 1982.
43. Thomas A, Muniandy K. Polymer 1987;28:408–415.
44. Heng LY, Toth K, Hall EA. H. Talanta 2004;63:73–87.
45. Lindner E, Gyurcsanyi RE. J. Solid-State Electrochem. 2008in press
46. Fogt EJ, Untereker DF, Norenberg MS, Meyerhoff M. Anal. Chem 1985;57:1995–1998. [PubMed: 3929646]
47. Grygolowicz-Pawlak E, Plachecka K, Brzozka Z, Malinowska E. Sens. Actuators B 2007;123:480–487.
48. Lai CZ, Fierke MA, Stein A, Buhlmann P. Anal. Chem 2007;79:4621–4626. [PubMed: 17508716]

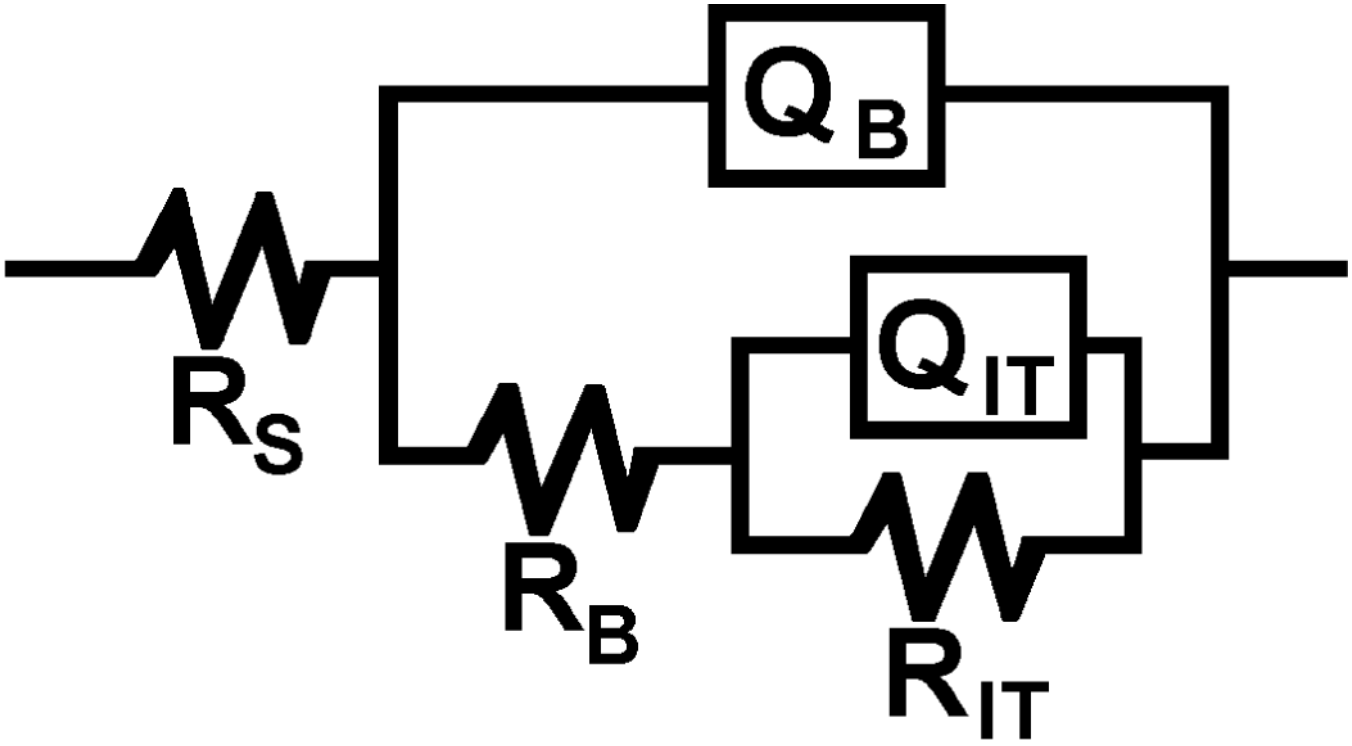

Figure 1.
Equivalent circuit used in the fitting of EIS data, noting the following definitions for the circuit elements: 1) R_S is the solution resistance; 2) R_B and Q_B are the resistance and constant phase element for the bulk membrane, respectively; 3) R_{IT} and Q_{IT} are the resistance and constant phase element for the ion transfer process, respectively.

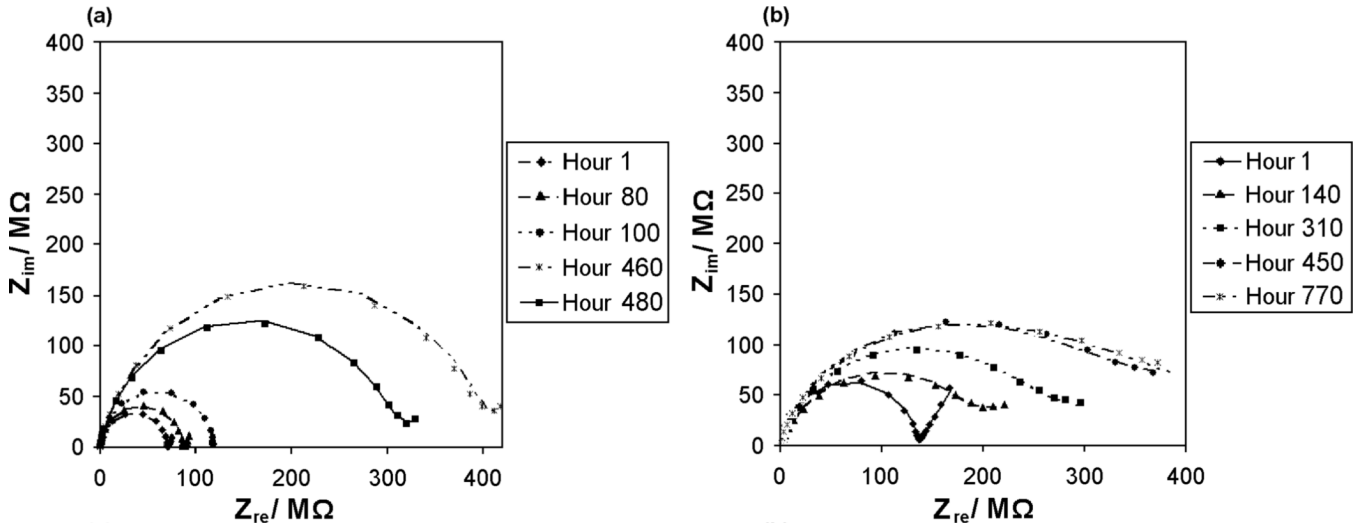

Figure 2.
EIS Nyquist plots for the copolymer system in the absence (a) and presence (b) of a POT solid-contact.

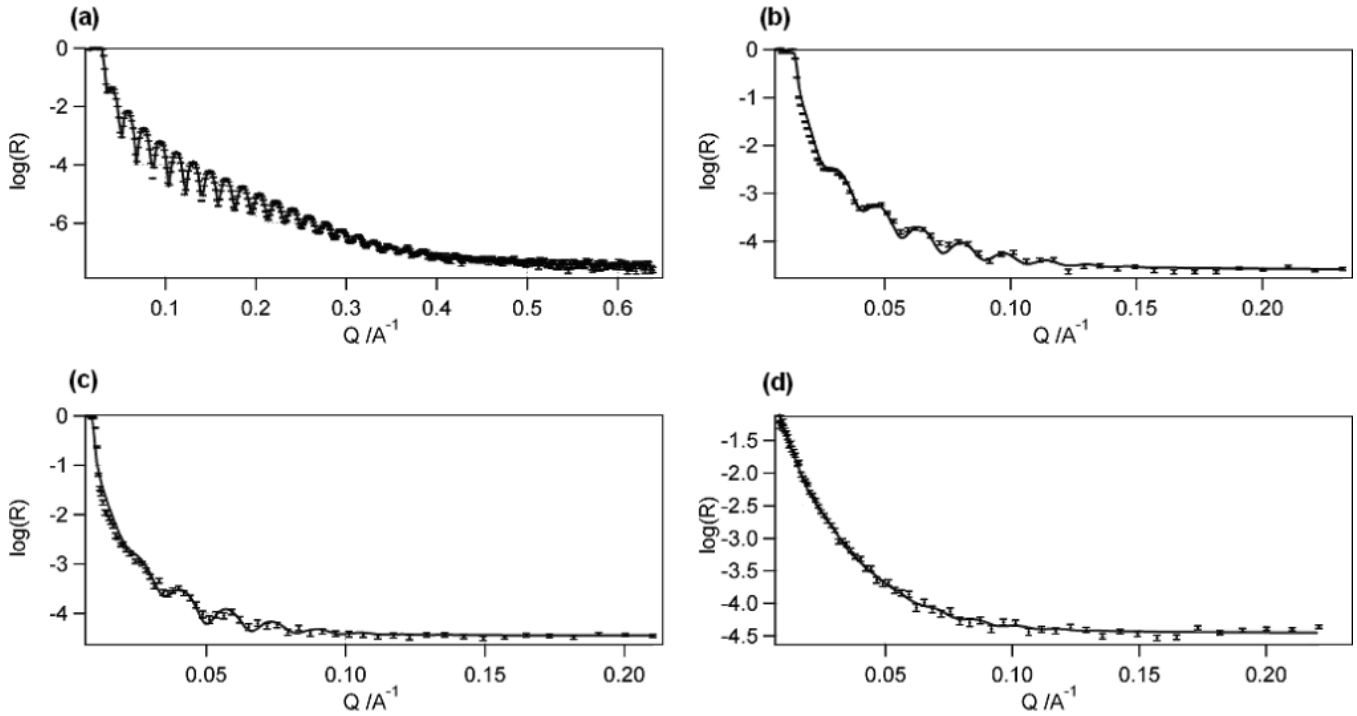

Figure 3.

(a) XR reflectivity curve of the POT/copolymer solid contact ISE taken in air. Figure also shows, as well as NR reflectivity curves for the POT/copolymer solid-contact ISE exposed to electrolytes in (b) D_2O, (c) D_2O/H_2O and (d) H_2O. Note, R is the neutron reflectivity, and Q is the scattering vector that is inversely proportional to the size of nanoscatterer.

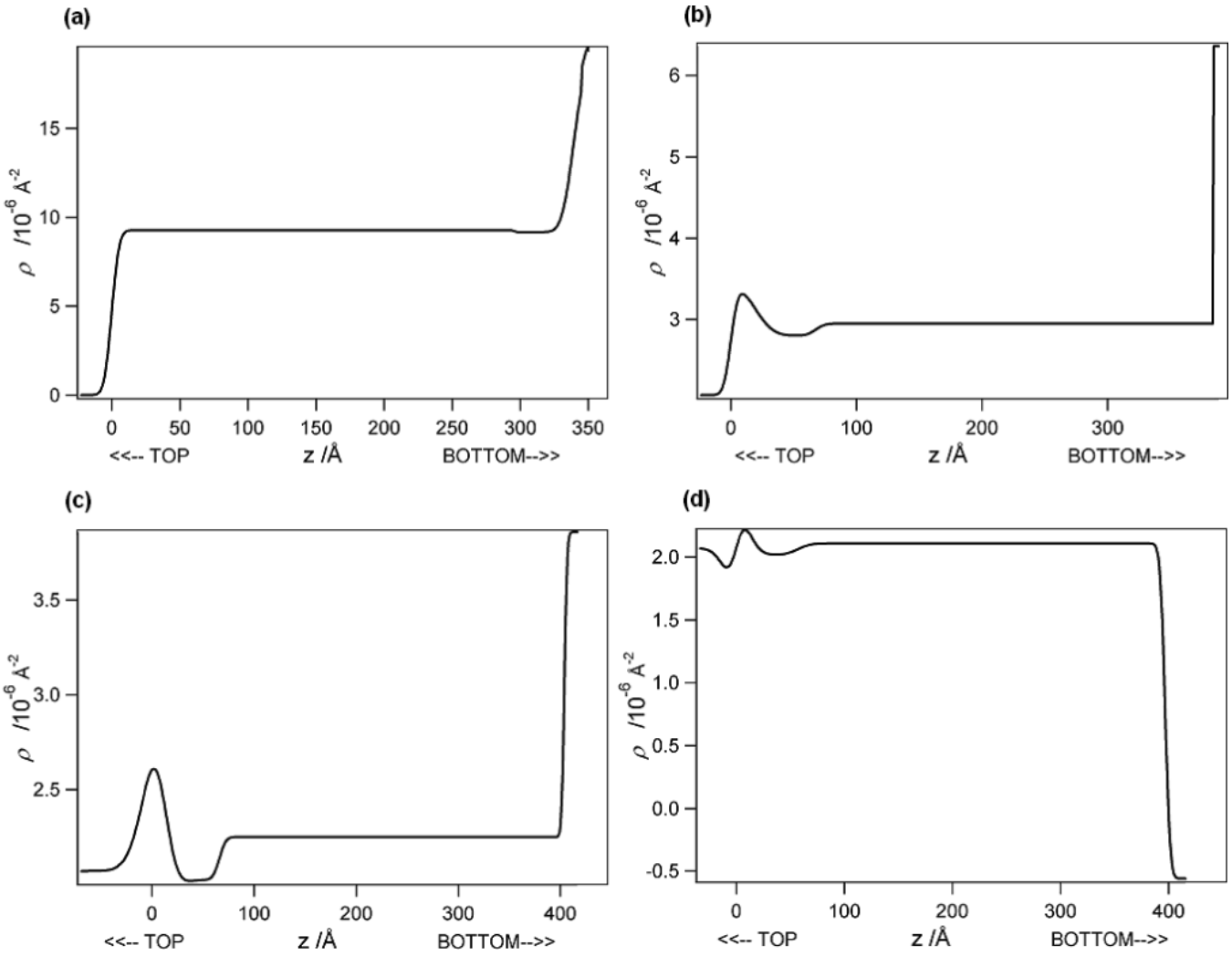

Figure 4.

(a) XR SLD plot for the POT/copolymer solid contact ISE measured in air, as well as SLD profiles for NR when the POT/copolymer solid contact ISE is exposed to (b) D_2O, (c) D_2O/H_2O and (d) H_2O, noting that ρ represents the SLD.

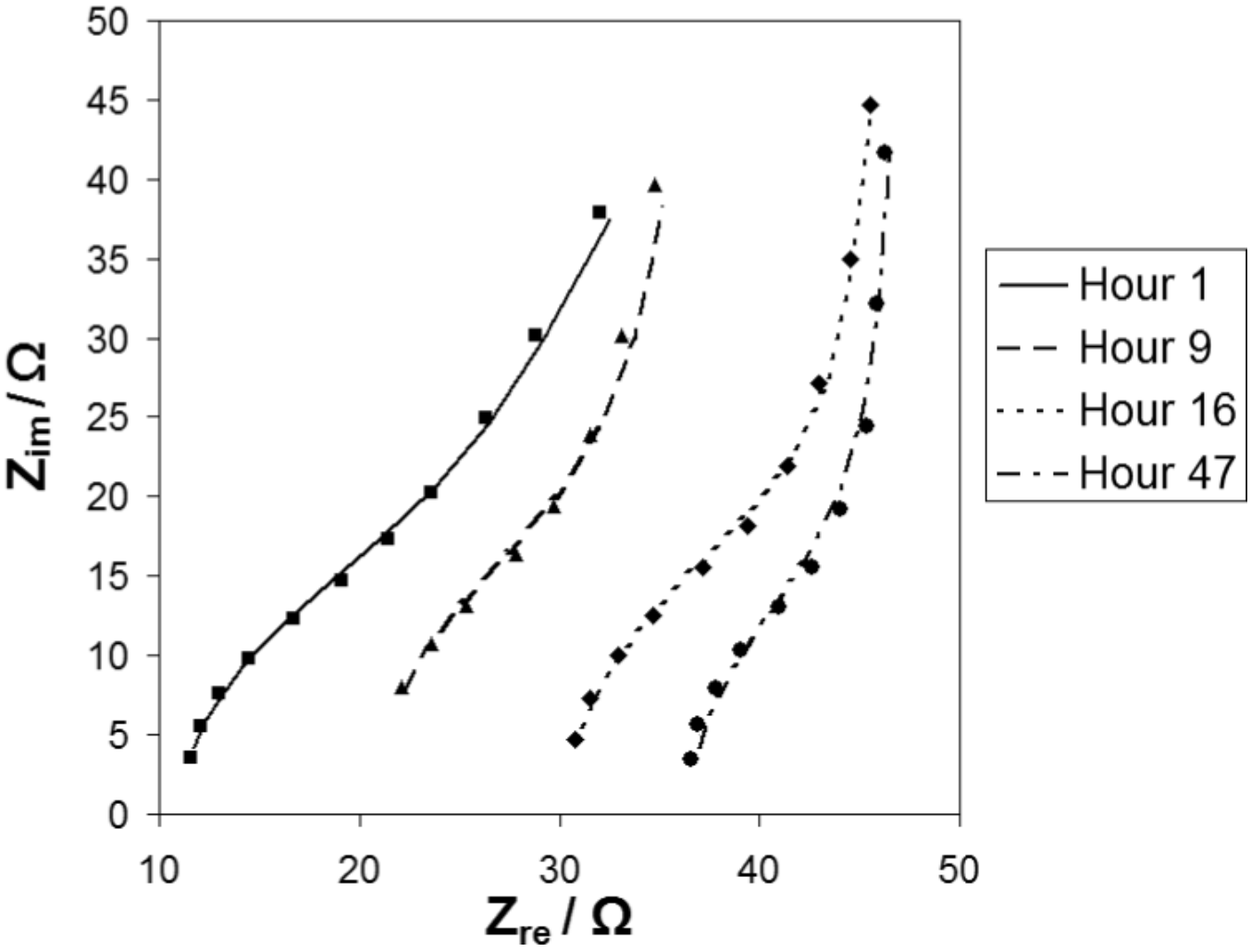

Figure 5.
EIS Nyquist plots for the molecularly thin POT/copolymer solid-contact ISE as a function of exposure to aqueous electrolyte in the EIS/NR experiment.

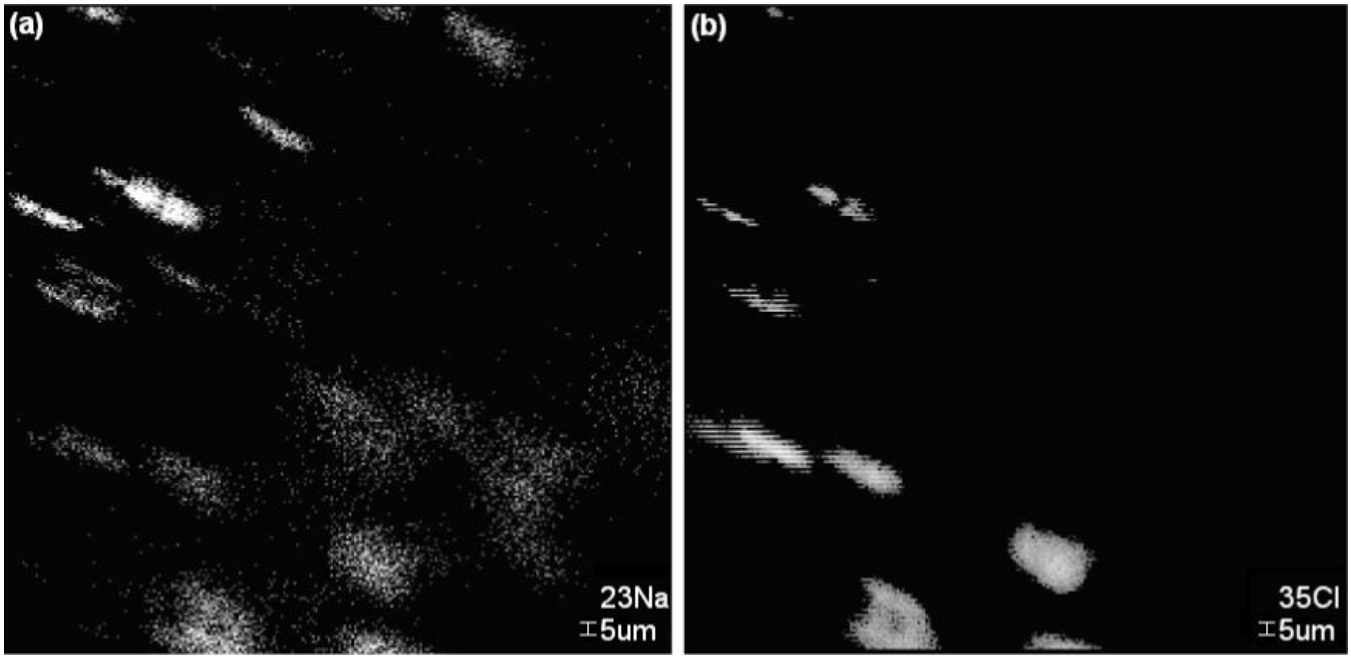

Figure 6.
SIMS (a) ^{23}Na and (b) ^{35}Cl negative ion chemical maps of the gold/copolymer membrane interface for a copolymer ISE exposed to 0.1 M NaCl for 48 hours.

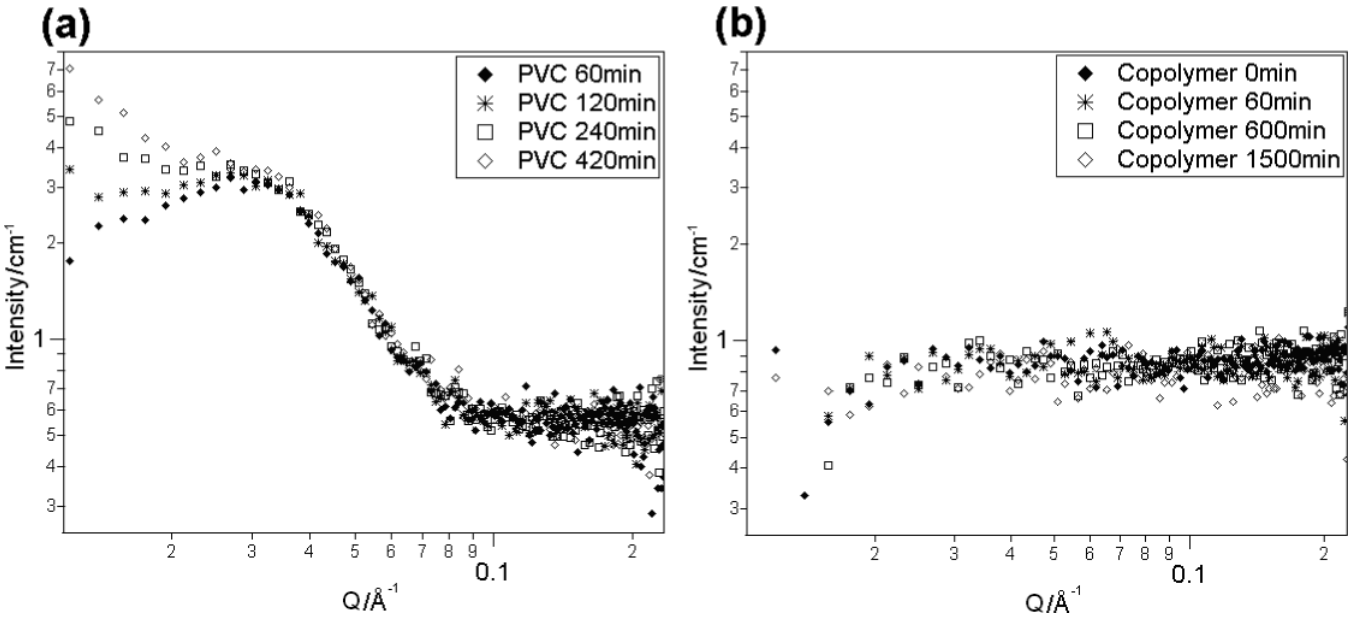

Figure 7.

SANS scattering curves for a) PVC ISE bathed in acid solution, and (b) a copolymer bathed in acid solution, noting that 1/cm represents the normalized neutron scattering intensity and Q is the scattering vector that is inversely proportional to the size of the nanoscatterer.

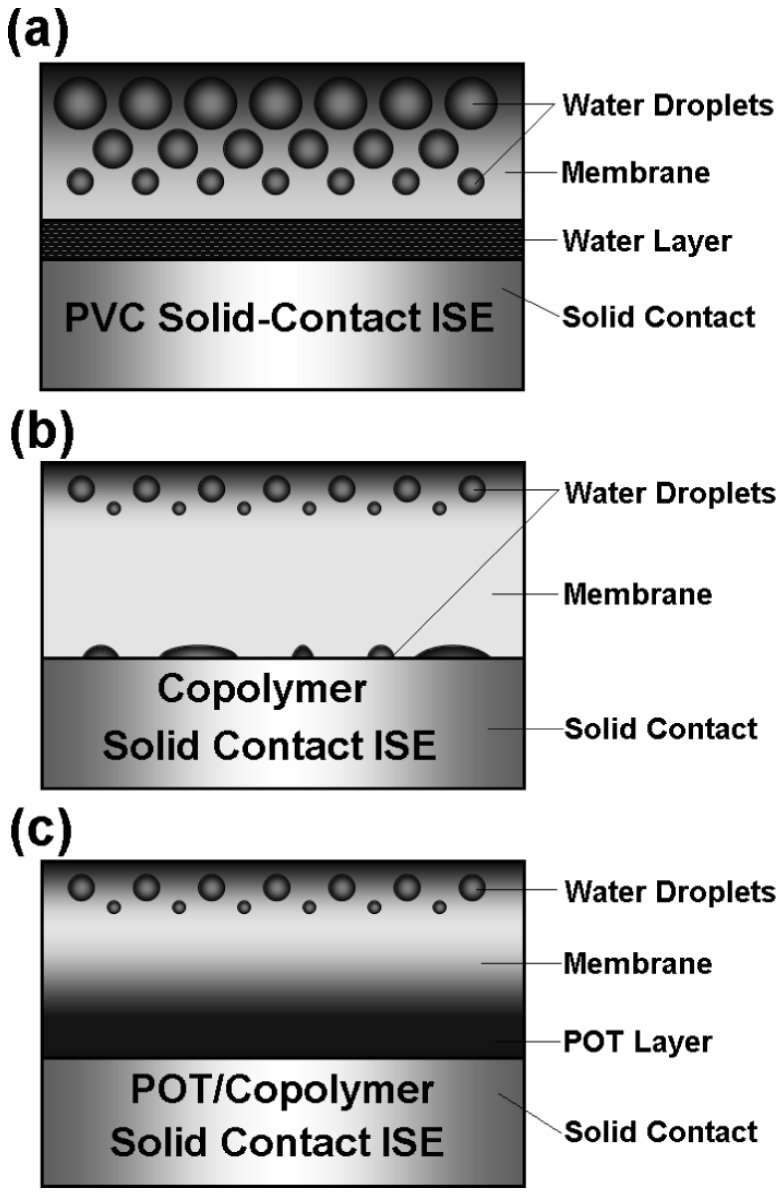

Figure 8.
Physical depictions of various solid-contact ISEs: a) PVC system with well-defined water layer; b) copolymer system with less water uptake and pools of water forming at the buried interface, noting that the black shaded areas represent water inclusions in the ISEs such as water nanodroplets (spheres), water "pockets and pools" (hemispheres or partial spheres) and water layers (a continuous layer); (c) copolymer/POT solid-contact ISE showing the absence of a water layer at the buried interface, noting that the three layers (from top to bottom) are pure copolymer ion-selective membrane, the diffuse layers of POT and copolymer membrane and finally the pure POT ion-to-electron transducer layer.

Table 1

EIS equivalent circuit fitted parameters for a CWE copolymer ISE, as determined using the equivalent circuit presented in Figure 1.

	R_s (Ω)	Q_B (10^{-10} $\Omega^{-1}s^n$)	n_1	R_B (MΩ)	Q_{IT} (10^{-7} Ω^{-1} s^n)	n_2	R_{IT} (MΩ)
Hour 1	30.0	3.22	0.90	71	10.7	0.90	30
Hour 80	30.0	3.29	0.95	88	9.0	0.73	40
Hour 100	30.0	3.23	0.95	119	7.0	0.90	71
Hour 460	30.0	6.00	0.80	411	6.9	0.80	90
Hour 480	30.0	6.49	0.80	302	0.9	0.80	98

Table 2

EIS equivalent circuit fitted parameters for a POT solid-contact copolymer ISE, as determined using the equivalent circuit presented in Figure 1.

	R_s(Ω)	Q_B(10^{-9} Ω^{-1} s^n)	n_1	R_B (MΩ)	Q_{IT} (10^{-8} Ω^{-1} s^n)	n_2	R_{IT} (MΩ)
Hour 1	30.0	2.58	0.93	137	6.0	0.80	227
Hour 140	30.0	1.51	0.80	198	7.9	0.80	230
Hour 310	30.0	1.43	0.82	238	8.7	0.80	321
Hour 450	30.0	1.84	0.81	340	19.7	0.70	523
Hour 770	30.0	1.99	0.81	345	30.0	0.90	724

Table 3

NR fitted parameters using a two film model for water impregnated copolymer, and an amalgam of POT and copolymer.

Contrast	Copolymer Thickness (Å)	SLD (10^{-6}Å^{-2})	Roughness (Å)	POT Thickness (Å)	SLD (10^{-6}Å^{-2})	Roughness (Å)
XR in air	295.84	9.27	4.32	42.94	9.17	1.18
NR in D_2O	316.50	2.95	5.89	48.14	2.80	11.26
NR in D_2O/H_2O	337.97	2.25	5.00	53.96	2.03	10.00
NR in H_2O	339.89	2.11	9.06	56.35	2.02	11.53

Table 4

EIS equivalent circuit fitted data for the molecularly thin POT/copolymer solid-contact ISE explored simultaneously using EIS/NR.

	$R_s(\Omega)$	$Q_B(\mu\Omega^{-1} s^n)$	n_1	$R_B(\Omega)$	Q_{IT} (10^{-5} $\Omega^{-1} s^n$)	n_2	R_{IT} (kΩ)
Hour 1	11.2	19.10	0.80	29	16.4	0.80	5
Hour 9	19.0	59.70	0.80	40	8.6	0.80	54
Hour 16	30.0	53.70	0.80	41	8.4	0.98	72
Hour 47	35.9	73.60	0.80	41	8.0	0.80	90

Table 5

EIS equivalent circuit fitted data for the molecularly thin copolymer CWE ISE studied simultaneously using EIS/NR.

	$R_s(\Omega)$	Q_B (10^{-5} Ω^{-1} s^n)	n_1	$R_B(\Omega)$	Q_{IT} (10^{-5} Ω^{-1} s^n)	n_2	R_{IT} (kΩ)
Hour 3	12.3	14.10	0.80	37	30.4	0.80	11
Hour 13	15.7	6.78	0.80	44	8.0	0.80	38
Hour 31	19.0	5.02	0.81	44	6.2	0.80	51
Hour 49	23.5	7.03	0.80	33	8.0	0.80	69